

Selection of generalized component modes for modally reduced flexible multibody systems

Andreas Zwölfer¹ and Johannes Gerstmayr¹

¹*Department of Mechatronics, University of Innsbruck {andreas.zwoelfer, johannes.gerstmayr}@uibk.ac.at*

ABSTRACT — *Increasing industrial demands on reliability and efficiency require advanced simulation models of dynamical systems. Virtually all engineering systems are assemblies made out of multiple components which interact with each other during operation. The forces required to execute desired motions are associated with stresses, noise and vibrations, which is why, flexible multibody simulations are inevitable for accurate predictions. However, most finite element models of relevant engineering problems contain a huge number of degrees of freedom, that cannot be simulated within a reasonable amount of time without employing model reduction techniques. Generalized component mode synthesis (GCMS) is a promising alternative to existing flexible multibody formulations, since it preserves a linear configuration space, leading to a constant mass and co-rotated stiffness matrix and no quadratic velocity vector. In the GCMS framework, the deformation is approximated by a linear combination of component modes generated from original finite element eigenmodes and undeformed nodal coordinates. The emerging reduction matrix is in many cases ill-conditioned due to linear dependencies of the GCMS modes and may introduce large errors or even lead to unsolvable problems. However, the problem of linearly dependent GCMS modes has not received much attention in the available literature despite its importance. Hence, the current contribution sheds some light on this problem inherently present in the formulation and gives suggestions how to handle the linear dependencies appropriately. The new findings are illustrated by numerical experiments of simple extruded bodies with different cross-sections and a crankshaft.*

1 Introduction

Increasing industrial demands on reliability and efficiency of modern moving engineering devices require advanced modelling techniques during the design process. At present time, virtually all such engineering systems are assemblies and, hence, made out of multiple components, which interact with each other during operation. The forces required to execute desired motions are associated with stresses, noise and vibrations of the bodies in the system. Thus, it is insufficient to model multibody systems as rigid bodies and extract boundary forces to perform subsequent standard finite element (FE) analyses. Flexible multibody simulations, where the system is spatially discretized using a finite number of elements, are, therefore, inevitable. However, most FE models of relevant engineering problems contain a huge number of degrees of freedom (DOFs), that cannot be simulated within a reasonable amount of time without employing model reduction techniques.

Generalized component mode synthesis (GCMS) [1] is a promising efficient alternative to existing flexible multibody system dynamics formulations, such as the floating frame of reference formulation (FFRF), since it preserves a linear relationship between the displacement field and the DOFs of the considered domain, yielding a constant mass matrix and a trivial quadratic velocity vector, which is not the case for the FFRF [2, p. 185] implemented in most commercial flexible multibody simulation packages. Moreover, it is a very generic formalism, easily applicable to any multibody system subjected to large reference motion, but small deformations of the individual components, which is the case for the majority of engineering systems, such as vehicles, robots and aircraft, since large deformations severely impair or even destruct the system and are, therefore, usually unwanted.

Both, the FFRF as well as the GCMS approximate the flexible deformation by a linear combination of component modes. In the case of the FFRF, the component modes are, for example, the eigenmodes of vibration limited to the frequency range of interest, or a combination of eigen- and static modes, see the pioneering work of [3]. If the deformation is approximated by vibration modes, the reduction matrix containing column-wise the eigenmodes is well-conditioned, since the eigenvectors are linearly independent [4, p. 158] even for repeated eigenvalues, since the Degeneracy theorem [5, p. 72] allows the generalization of the orthogonality of the eigenvectors in the metrics of the FE mass and stiffness matrices in the case of repeated eigenvalues. Hence, the reduction matrix of the component mode synthesis FFRF does not introduce numerical errors; in fact, the condition number is close to one if the eigenvectors are displacement normalized, for example, smaller than 1.4 for all hereinafter analysed models. Whereas, the GCMS reduction matrix is in many cases ill-conditioned, for example, in the order of 10^6 to 10^{17} for the hereinafter analysed beam-like models, because of linearly dependent GCMS modes that may arise due to the special structure of the reduction basis Φ , see Sec. 2.1. It is well known, that such linear dependencies can even lead to unsolvable problems, since they preclude the factorization of the system Jacobian impossible.

There is past work concerned with a rigorous mathematical derivation of the GCMS modes and equations of motion [1, 6], whereas [7] shows how the idea may be employed without modal reduction. Also the GCMS formulation has been successfully applied to engineering problems, such as fluid-structure interaction [8] and machine parts with large rotations about one axis only [9], and was extended by means of a nullspace projection approach [10] as well as the global modal parametrization [11]. However, the problem of linear dependencies has not received much attention, despite its importance. The issue was marginally reported in [1, 6], but has not been addressed in the available literature. Furthermore, it has been believed that these dependencies can only arise for symmetric problems, which is, as shown in the present paper, in general not true. Hence, the aim of this contribution is to shed some light on this problem inherently present in the GCMS formulation and give suggestions how to handle these linear dependencies appropriately.

The rest of the paper is structured as follows: Sec. 2 is devoted to the configuration space, where the GCMS modes are defined and the linear relationship between the global nodal displacements and DOFs is illustrated, as well as to a compact derivation of the GCMS equations of motion with a Lagrangian formulation for a general spatially discretized mechanical system (in contrast to the original continuum mechanics based derivation reported in the literature). Sec. 3 presents a short note on the mathematics of linear dependencies and how to handle them, which is required to analyse and eliminate linear dependencies in the GCMS reduction matrix. Sec. 4 and Sec. 5 analyse the linear dependencies of the flexible part of the reduction matrix and between the flexible and the rigid body motion part, respectively, with the help of simple FE beam-like models. Sec. 6 applies the presented theory to a FE model of a crankshaft of a two-cylinder reciprocal combustion engine and Sec. 7 gives a step-by-step strategy how to handle the linear dependencies of the GCMS reduction matrix, followed by a conclusion and suggestions for future research.

2 Generalized Component Mode Synthesis

2.1 Reduction basis

The GCMS formulation exploits a modal superposition reduction method, where the flexible deformation is approximated by a linear combination of vibration modes to reduce the system size from a large number of DOFs to a significantly smaller one. This, of course, restricts its applicability to problems where the deformation of the components remains linear within each body frame. The so called generalized component modes, or GCMS shape vectors, account not only for large rigid body motion (translation & rotation), but also represent the deformation modes in any possible orientation, leading to a linear configuration space. However, the linear relationship between the global displacements and the DOFs, i.e. GCMS coordinates, is obtained at the expense of a in general nine-fold increase in the number of flexible modal coordinates, i.e. nine flexible GCMS coordinates per original natural mode of vibration ϕ_m of the bodies in the system. Each flexible GCMS coordinate is associated with one GCMS mode generated from original eigenmodes. To obtain the flexible GCMS shape vectors, the original eigenmodes are split into three vectors containing only the displacements in either the 1, 2 or 3 coordinate direction,

respectively, and zeros elsewhere, at first. Subsequently, the displacements in the individual coordinate directions are applied to the other two coordinate directions, yielding nine generalized modes per original eigenmode, see Eq. (6). To illustrate this procedure, consider a simple hypothetical example of one eigenmode of a FE model with only one node and three DOFs:

$$\underbrace{\begin{bmatrix} \phi_m^1 \\ \phi_m^2 \\ \phi_m^3 \end{bmatrix}}_{\text{eigenmode}} \longrightarrow \underbrace{\begin{bmatrix} \phi_m^1 & 0 & 0 & \phi_m^2 & 0 & 0 & \phi_m^3 & 0 & 0 \\ 0 & \phi_m^1 & 0 & 0 & \phi_m^2 & 0 & 0 & \phi_m^3 & 0 \\ 0 & 0 & \phi_m^1 & 0 & 0 & \phi_m^2 & 0 & 0 & \phi_m^3 \end{bmatrix}}_{\text{corresponding set of nine GCMS modes}} \quad (1)$$

The formal rules to generate the translational, rotational and flexible GCMS shape vectors are explicitly stated in Eqs. (4) to (6); it is shown in [1] that the GCMS modes may be obtained by mainly rearranging the equations during the derivation of the component mode synthesis FRFF.

The reduced set of GCMS coordinates \mathbf{q} is related to the full set of FE nodal coordinates \mathbf{c} via

$$\mathbf{c} \approx \Phi \mathbf{q} \quad \text{with} \quad \dim(\mathbf{q}) \ll \dim(\mathbf{c}), \quad (2)$$

where $\dim(\dots)$ denotes the dimension of the quantity in brackets; the GCMS reduction matrix Φ contains the translational $\Phi_t \in \mathbb{R}^{3N_n \times 3}$, the rotational $\Phi_r \in \mathbb{R}^{3N_n \times 9}$ and the flexible $\Phi_f \in \mathbb{R}^{3N_n \times 9N_m}$ GCMS shape vectors, i.e.

$$\Phi = [\Phi_t \quad \Phi_r \quad \Phi_f], \quad (3)$$

where

$${}^t\phi^l = [e_l^T \quad e_l^T \quad \dots \quad e_l^T]^T, \quad (4)$$

$${}^r\phi^{kl} = [X_k^1 e_l^T \quad X_k^2 e_l^T \quad \dots \quad X_k^{N_n} e_l^T]^T, \quad (5)$$

$${}^f\phi_m^{kl} = [\phi_m^k e_l^T \quad \phi_m^{k+3} e_l^T \quad \dots \quad \phi_m^{k+3(N_n-1)} e_l^T]^T, \quad (6)$$

with $k, l = 1, 2, 3$ and $m = 1, \dots, N_m$ represent the columns of Φ_t , Φ_r and Φ_f , respectively. In Eqs. (4) to (6), $e_l \in \mathbb{R}^3$ denotes the orthonormal set of Cartesian base vectors, X_k^i the i -th nodal coordinate of the k -th coordinate direction of the undeformed FE model, ϕ_m^k denotes the k -th component of the m -th natural eigenmode of vibration and N_n as well as N_m the number of nodes and eigenmodes, respectively¹. The GCMS coordinates \mathbf{q} are, of course, also partitioned in a similar manner as the GCMS reduction matrix Φ , see Eq. (3), in translational, rotational and flexible GCMS coordinates, i.e.

$$\mathbf{q} = [\mathbf{q}_t^T \quad \mathbf{q}_r^T \quad \mathbf{q}_f^T]^T. \quad (7)$$

As already mentioned, the GCMS shape vectors arise from rearranging the equations during the derivation of the FRFF. However, the origin of the GCMS shape vectors is not the object of the present paper and the interested reader is referred to [1] for a rigorous mathematical derivation of the reduction matrices, where the GCMS formalism is also contrasted with the component mode synthesis FRFF.

2.2 Equations of motion

In this section the GCMS equations of motion, originally derived on the basis of the FRFF via a continuum mechanics approach, are derived in a compact way starting in the already spatially discretized domain. The semi-discretized equations of motion are derived via Lagrange's equation, i.e.

$$\frac{d}{dt} \left(\frac{\partial L}{\partial \dot{\mathbf{q}}^T} \right) - \frac{\partial L}{\partial \mathbf{q}^T} = \mathbf{0}, \quad (8)$$

¹Note, for a 3-dimensional FE model discretized with continuum elements, the total number of DOFs is equal to $3N_n$.

with the (modified) Lagrangian L [12, p. 141] for a general mechanical system defined as

$$L = T - V - W + \boldsymbol{\lambda}^T \mathbf{g}, \quad (9)$$

where W denotes the work done by applied nodal forces, $\boldsymbol{\lambda}$ the vector of Lagrange multipliers and $\mathbf{g} = \mathbf{0}$ the vector of holonomic constraint equations. The internal potential energy, i.e. the strain energy V , the kinetic energy T and W for a classical FE model read

$$V = \frac{1}{2} \bar{\mathbf{c}}^T \mathbf{K} \bar{\mathbf{c}}, \quad (10)$$

$$T = \frac{1}{2} \dot{\mathbf{c}}^T \mathbf{M} \dot{\mathbf{c}} \quad (11)$$

and

$$W = \mathbf{c}^T \mathbf{f}, \quad (12)$$

where $\bar{\mathbf{c}}$ denotes the FE nodal displacements in the body frame, \mathbf{K} and \mathbf{M} the linear FE stiffness and mass matrices, respectively, and \mathbf{f} the applied FE nodal forces. Note, Eq. (10) is only valid for linear FE models (“small strain” tensor), i.e. in the body frame, however, the GCMS formulation accounts for large rigid body translation and rotation and is therefore a geometrically non-linear formalism even though the deformations remain small. Hence, it is not possible to substitute the global nodal displacements \mathbf{c} of Eq. (2) directly in the expression of the strain energy for a classical linear FE model, which is why, Eq. (10) is stated in terms of $\bar{\mathbf{c}}$, i.e. only the flexible part of \mathbf{q} contributes to the strain energy. The GCMS coordinates associated with the flexible deformation \mathbf{q}_{flx} are calculated via

$$\mathbf{q}_{\text{flx}} = [\mathbf{0}^T \quad (\mathbf{q}_r - \mathbf{q}_r^*)^T \quad \mathbf{q}_f^T]^T, \quad (13)$$

where \mathbf{q}_r^* denotes proper rotational coordinates obtained by an appropriate orthogonalization procedure (Gram-Schmidt) and are therefore a function of \mathbf{q}_r , i.e. no additional DOFs are introduced here. Note, the rotational \mathbf{q}_r and flexible \mathbf{q}_f GCMS coordinates do not correspond directly to rotational and flexible displacements only, since \mathbf{q}_r may also contain stretch and shear deformations [1]. Hence, the global flexible displacement \mathbf{u}_f reads

$$\mathbf{u}_f = \mathbf{N} \boldsymbol{\Phi} \mathbf{q}_{\text{flx}}, \quad (14)$$

where \mathbf{N} denotes the FE shape function matrix. The flexible displacement in the body frame $\bar{\mathbf{u}}_f$ is given by

$$\bar{\mathbf{u}}_f = \mathbf{N} \bar{\mathbf{c}}, \quad (15)$$

according to standard FE theory [13], and the absolute (global) and local flexible displacements are related via

$$\mathbf{u}_f = \mathbf{A} \bar{\mathbf{u}}_f, \quad (16)$$

as known from the well-established FFRF [2, p. 185]. Therefore,

$$\bar{\mathbf{c}} = \mathbf{A}_{\text{bd}}^T \boldsymbol{\Phi} \mathbf{q}_{\text{flx}} = \boldsymbol{\Phi} \mathbf{A}_{\text{bd}}^T \mathbf{q}_{\text{flx}}, \quad (17)$$

since

$$\mathbf{A} \mathbf{N} = \mathbf{N} \mathbf{A}_{\text{bd}} \quad \text{and} \quad \mathbf{A}_{\text{bd}}^T \boldsymbol{\Phi} = \boldsymbol{\Phi} \mathbf{A}_{\text{bd}}^T, \quad (18)$$

where $\mathbf{A}_{\text{bd}} = \text{diag}(\mathbf{A}, \dots, \mathbf{A})$ denotes a block-diagonal matrix with the rotation matrix $\mathbf{A} \in \mathbb{R}^{3 \times 3}$ (relating the global and local frame) on its diagonal. The matrices in Eq. (18) commute, since the reduction matrix $\boldsymbol{\Phi}$ and the FE shape function matrix \mathbf{N} consist of multiples of the 3 by 3 identity matrix, see Eqs. (3) to (6) and standard FE literature such as [13]. Note, the size of the block-diagonal rotation matrix \mathbf{A}_{bd} changes if the order of multiplication is changed, such that a proper matrix multiplication is well defined, i.e. matching dummy indices.

Substituting Eq. (17) and Eq. (2) into Eq. (10) and Eq. (11), respectively, yields the strain and kinetic energy in terms of the GCMS coordinates, i.e.

$$V = \frac{1}{2} \mathbf{q}_{\text{flx}}^T \mathbf{A}_{\text{bd}} \Phi^T \mathbf{K} \Phi \mathbf{A}_{\text{bd}}^T \mathbf{q}_{\text{flx}}, \quad (19)$$

$$T = \frac{1}{2} \dot{\mathbf{q}}^T \Phi^T \mathbf{M} \Phi \dot{\mathbf{q}}. \quad (20)$$

The equations of motion are then obtained by combining Eqs. (2), (8), (9), (12), (19) as well as Eq. (20) and carrying out differentiation with respect to \mathbf{q} , $\dot{\mathbf{q}}$ and t , which yields

$$\widehat{\mathbf{M}} \dot{\mathbf{q}} + \mathbf{A}_{\text{bd}} \widehat{\mathbf{K}} \mathbf{A}_{\text{bd}}^T \mathbf{q}_{\text{flx}} + \mathbf{f}_{\text{nl}} + \mathbf{G}^T \boldsymbol{\lambda} = \widehat{\mathbf{f}}, \quad (21)$$

with the reduced system matrices

$$\widehat{\mathbf{M}} = \Phi^T \mathbf{M} \Phi, \quad (22)$$

$$\widehat{\mathbf{K}} = \Phi^T \mathbf{K} \Phi, \quad (23)$$

the reduced vector of applied forces

$$\widehat{\mathbf{f}} = \Phi^T \mathbf{f} \quad (24)$$

and the constraint Jacobian

$$\mathbf{G} = \frac{\partial \mathbf{g}}{\partial \mathbf{q}}. \quad (25)$$

The non-linear term \mathbf{f}_{nl} in Eq. (21) reads

$$\mathbf{f}_{\text{nl}} = \mathbf{q}_{\text{flx}}^T \mathbf{A}_{\text{bd}} \widehat{\mathbf{K}} \frac{\partial \mathbf{A}_{\text{bd}}^T}{\partial \mathbf{q}^T} \mathbf{q}_{\text{flx}}, \quad (26)$$

and may be computed as [1]

$$\mathbf{f}_{\text{nl}} = \sum_{i,j=1}^3 \mathbf{q}_{\text{flx}}^T \mathbf{A}_{\text{bd}} \widehat{\mathbf{K}} \frac{\partial \mathbf{A}_{\text{bd}}^T}{\partial A_{ij}} \mathbf{q}_{\text{flx}} \frac{\partial A_{ij}}{\partial \mathbf{q}^T}, \quad (27)$$

where the partial derivative of \mathbf{A}_{bd}^T and of the components of the rotation matrix A_{ij} are Boolean matrices and vectors, respectively, and the non-linear term \mathbf{f}_{nl} is non-zero for the rotational GCMS coordinates \mathbf{q}_r only.

Eq. (21) reveals the advantages of the GCMS formulation over the FFRF and classic geometrically non-linear FE methods: the system matrices, \mathbf{M} and \mathbf{K} , remain constant during the whole simulation and need not to be assembled for each time step. This makes the method very efficient and superior in terms of computation time compared to other methods.

3 A short note on linear dependencies

3.1 Linear Dependence

As already pointed out in Sec. 1, a straight forward generation of Φ according to Eqs. (3) to (6) may lead to an ill-conditioned system due to linearly dependent GCMS shape vectors, which is why, this section is devoted to a short note on the mathematics of linear dependence.

The GCMS shape vectors φ_i , i.e. the columns of Φ , are said to be linearly dependent if

$$a_p^1 \varphi_1 + a_p^2 \varphi_2 + \dots + a_p^n \varphi_n = \mathbf{0}, \quad (28)$$

if the scalars a_p^i are not all zero; this may be written in matrix-vector notation as²

$$\Phi \mathbf{a}_p = \mathbf{0} \quad \text{where} \quad \Phi = [\varphi_1 \quad \varphi_2 \quad \dots \quad \varphi_n] \quad \text{and} \quad \mathbf{a}_p = \begin{bmatrix} a_p^1 \\ a_p^2 \\ \vdots \\ a_p^n \end{bmatrix}. \quad (29)$$

Hence, the GCMS shape vectors are linearly independent if the kernel (nullspace) of the GCMS reduction matrix contains only the zero vector, i.e. if $\text{null}(\Phi) = \{\mathbf{0}\}$.

3.2 Determine linear dependencies

3.2.1 Grammian

Since Φ is in general not square, we cannot use its determinant $\det(\dots)$ as an indicator of linear dependence, however, if we multiply Eq. (29) from the left with Φ^T we see that $\text{null}(\Phi) = \text{null}(\Phi^T \Phi)$. Hence, $\det(\Phi^T \Phi)$, the well known Grammian, indicates whether the GCMS shape vectors are linearly independent or not, i.e. $\det(\Phi^T \Phi) \neq 0 \Rightarrow \Phi \mathbf{a}_p \neq \mathbf{0}$ if $\mathbf{a}_p \neq \mathbf{0}$. Since we are dealing with real world problems numerically, it is unlikely that the Grammian of the GCMS matrix is exactly equal to zero if linear dependencies exist. Hence, one has to determine a threshold, under which the Grammian is considered as zero.

The Grammian of a matrix with entries smaller than one, which is usually the case for the main part (Φ_f) of the reduction matrix, is much smaller than one, for example, $\det[(\varepsilon \mathbf{I}_n)^T (\varepsilon \mathbf{I}_n)] = \varepsilon^{2n} \approx 0$ for $\varepsilon \ll 1$ even though the columns of $(\varepsilon \mathbf{I}_n)$ are linearly independent ($\mathbf{I}_n \in \mathbb{R}^{n \times n}$... identity matrix). Also, the Grammian is not invariant to scaling, i.e. $\det[(b\Phi)^T (b\Phi)] \neq \det(\Phi^T \Phi)$ for some scalar b . These properties make the Grammian critical and non-practical to use as an indicator for linear dependence of Φ .

Thus, $\det(\Phi^T \Phi)$ can only act as an indicator, and as shown here a not reliable one, whether columns of Φ are linearly dependent or not, but no information about the nature of the dependencies, i.e. which columns are in what way linearly dependent, is gained.

3.2.2 Singular-value decomposition

To reveal information about the nature of the linear dependencies, the singular value decomposition (SVD) of Φ , i.e. the matrix decomposition

$$\Phi = U \Sigma V^T, \quad (30)$$

where $U \in \mathbb{R}^{3N_n \times 3N_n}$ and $V \in \mathbb{R}^{(12+9N_m) \times (12+9N_m)}$ are orthogonal³ matrices whose columns are the left \mathbf{u}_i and right \mathbf{v}_i singular vectors, respectively, and $\Sigma \in \mathbb{R}^{3N_n \times (12+9N_m)}$ is a rectangular diagonal matrix with the singular values σ_i on its diagonal, may be employed to determine the nullspace of Φ . Right multiplying Eq. (30) with V yields

$$\begin{aligned} \Phi V &= U \Sigma, \\ \Phi [v_1 \quad v_2 \quad \dots \quad v_{12+9N_m}] &= [u_1 \quad u_2 \quad \dots \quad u_{3N_n}] \Sigma, \\ [\Phi v_1 \quad \Phi v_2 \quad \dots \quad \Phi v_{12+9N_m}] &= [\sigma_1 u_1 \quad \sigma_2 u_2 \quad \dots \quad \sigma_{3N_n} u_{3N_n}], \end{aligned} \quad (31)$$

with $12 + 9N_m \leq 3N_n$. The last equality in Eqs. (31) follows from the fact that right multiplying a matrix with a diagonal matrix is equal to multiplying the columns of that matrix with the diagonal entries of the diagonal matrix. Eq. (31) shows that the right singular values v_p corresponding to vanishing singular values σ_p are elements of the nullspace of Φ . Hence, the components of v_p are the coefficients a_p^i of Eq. (28), i.e. $v_p = \mathbf{a}_p$, compare Eq. (29) with (31).

²Note, the subscript p should indicate that the vector \mathbf{a} is not unique.

³Note, U and V are in general unitary matrices, however, since Φ is real, U and V are also real.

3.2.3 Matrix condition number

The SVD is not only useful to determine the nullspace of a matrix, but may be also used to define the condition number $\text{cond}(\Phi)$ of a matrix, which determines how accurately a linear system of equations can be solved. The condition number may be seen as an amplification of error, and one has to expect to loose $\log_{10}[\text{cond}(\Phi)]$ digits of accuracy [14, p. 95]. If the condition number is small, the matrix is said to be well-conditioned, otherwise ill-conditioned.

For a rectangular matrix, such as $\Phi \in \mathbb{R}^{3N_n \times (12+9N_m)}$ with $12 + 9N_m \leq 3N_n$, the condition number is in general defined as [14, p. 95]

$$\text{cond}(\Phi) = \|\Phi\| \|\Phi^+\|, \quad (32)$$

where Φ^+ denotes the pseudoinverse; if $\|\dots\|$ denotes the 2-norm (Frobenius norm), Eq. (32) may be written as the ratio of the largest σ_{\max} to the smallest σ_{\min} singular value, see Eq. (31), i.e.

$$\text{cond}(\Phi) = \frac{\sigma_{\max}(\Phi)}{\sigma_{\min}(\Phi)}, \quad (33)$$

which links the SVD and the matrix condition number.

If the GCMS equations of motion, Eq. (21), are integrated with the Newmark method [15], the inverse of the Jacobian reads [6]

$$\mathbf{J}^{-1} = \mathbf{A}_{\text{bd}} (\Phi^T \mathbf{M} \Phi + \beta \tau^2 \Phi^T \mathbf{K} \Phi)^{-1} \mathbf{A}_{\text{bd}}^T, \quad (34)$$

with the Newmark parameter β [15] and the time increment τ . The condition number of the reduction matrix Φ is related to the condition of the Jacobian \mathbf{J} , which can be estimated by means of matrix norm relations [14, p. 17] and Eq. (32), but is also evident from numerical experiments. The condition number of the part of the Jacobian that needs to be factorized during time integration is between four to eight orders of magnitude higher than the condition number of the GCMS reduction matrix, which is why, it is essential to ensure that $\text{cond}(\Phi)$ is sufficiently small to prevent errors during simulation. A high condition number of the GCMS reduction matrix leads to an ill-conditioned system Jacobian and an inaccurate solution and must be, therefore, avoided.

3.2.4 Cosine similarity

A special case of linear dependence is whenever two columns of Φ are directly proportional to each other, i.e. $\varphi_i = b\varphi_j$ for some non-zero scalar b , which is the case for flexible GCMS shape vectors (the main part of Φ) contained in Φ_f .

Directly proportional columns fulfil the condition

$$\cos \theta_{ij} = \frac{\langle \varphi_i, \varphi_j \rangle}{|\varphi_i| |\varphi_j|} \approx \pm 1, \quad (35)$$

where the row i and column j indices of Φ correspond to the indices k , l and m of Eqs. (4) to (6) in the following manner:

$$i, j = 9(m-1) + 3(k-1) + l, \quad (36)$$

which also represents the order the GCMS modes appear in the reduction matrices Φ_t , Φ_r and Φ_f . $-1 \leq \cos \theta_{ij} \leq 1$ is a measure of similarity between two vectors and known as the Cosine similarity. A value of ± 1 indicates linear dependence, whereas 0 orthogonality. Note the similarity to the modal assurance criterion (MAC), usually used to determine the consistency between eigenmode shapes of vibration from experiments and FE models.

For the flexible part Φ_f of the reduction matrix it suffices to check the value of the Cosine similarity of two columns in turn, since numerical experiments revealed that linear combinations of the flexible GCMS shape vectors with more than two columns involved do not arise.

3.3 An illustrative example

As evident from Sec. 2.1, the GCMS reduction basis $\Phi \in \mathbb{R}^{3N_n \times (12+9N_m)}$ contains predominately flexible GCMS modes, which is why, the main part of the present paper is devoted to the investigation of the flexible part of the GCMS reduction matrix, since Φ_f accounts for the majority of the linear dependencies and high condition number in the first place.

In this section, a simple illustrative example of a 60 mm square-sectioned 900 mm long steel beam should illustrate the problem of linearly dependent flexible GCMS modes. Fig. 1 depicts the first two bending eigenmodes of vibration with their nine corresponding flexible GCMS modes. The GCMS modes are shown here with different scaling factors for better comparability. It is clear from the figure that the first three GCMS modes of the first and second bending eigenmodes are identical. Moreover, the fourth to sixth GCMS modes of these two eigenmodes are related by the factor of negative one and are therefore directly proportional. Likewise, the set of the first three GCMS modes within each bending eigenmode is directly proportional to the set of the second three GCMS modes, i.e. ${}^f\phi_m^{1l} \propto {}^f\phi_m^{2l}$ with $m = 1, 2$ and $l = 1, 2, 3$. Hence, it is also possible that linear dependencies arise within one GCMS mode set, as shown here.

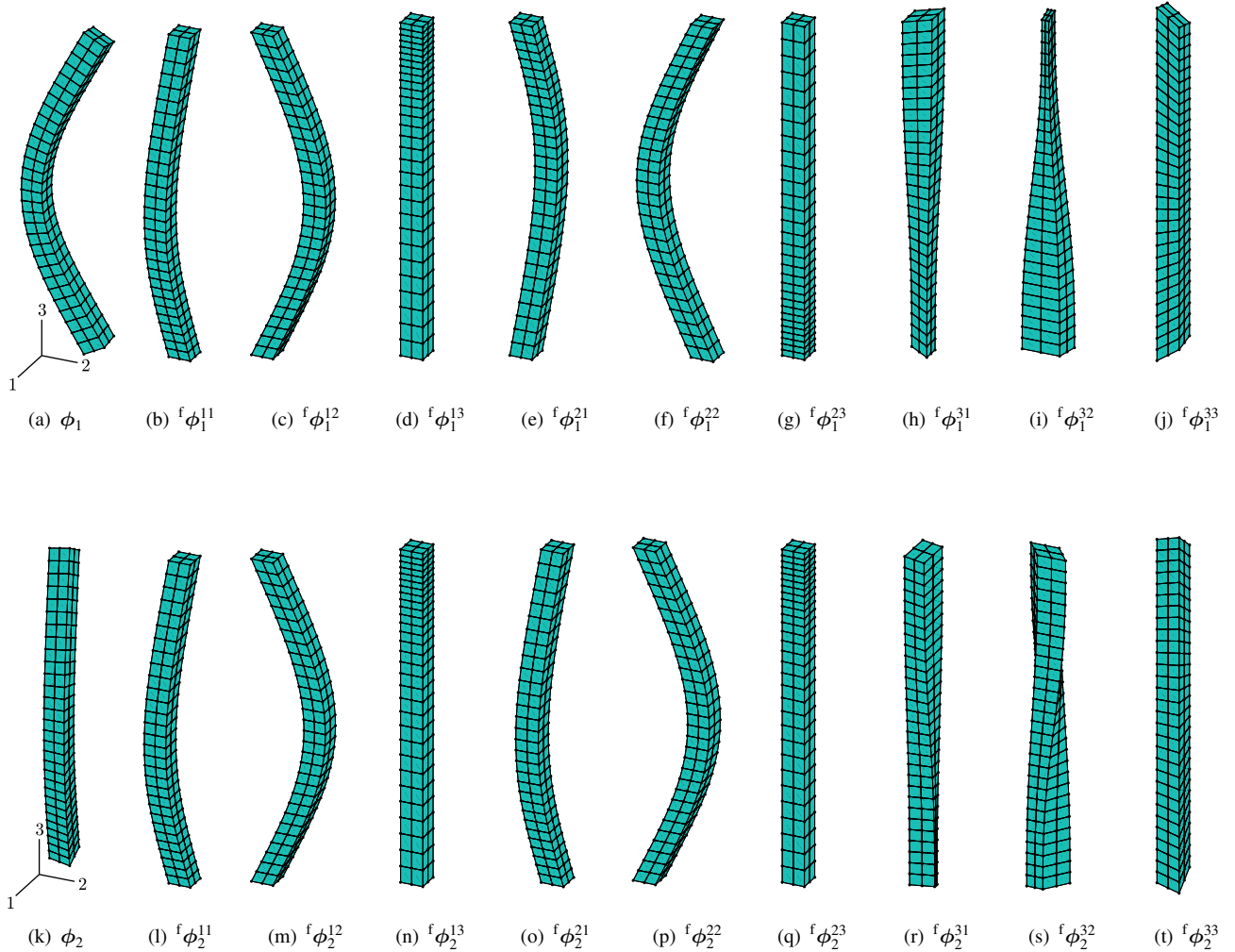


Fig. 1: First ϕ_1 and second ϕ_2 bending eigenmode of an unconstrained (no boundary conditions) square-sectioned steel beam and the nine corresponding flexible GCMS modes ${}^f\phi_1^{kl}$ and ${}^f\phi_2^{kl}$ according to Eq. (6), respectively.

These linear dependencies are attributed to the symmetric cross-section of the analysed beam and manifest themselves in a high condition number $\text{cond}(\Phi) = 9.51 \times 10^{17}$, and in a small Gramian $\det(\Phi^T \Phi) = 4.54 \times 10^{-35}$. Note, the first two eigenmodes of vibration form a repeated mode pair with equal eigenfrequencies, where the displacements in the 1- and 2-directions are simply “exchanged” for the first and second bending mode, since any axis through the centroid of a square cross-section is a principal (bending) axis. Consequently, only nine out of the full set of 18 GCMS modes are, in this case⁴, linearly independent and the system of equations with the initially $9N_m$ GCMS coordinates is again reduced significantly.

The degree of linear dependence of the flexible GCMS shape vectors is dictated by the value of $\cos \theta_{ij}$, see Eq. (35) and Sec. 3.2.4. The Cosine similarity may be represented as a 2-dimensional array of numbers and visualized with a color array, see for example the plot of $\cos \theta_{ij}$ of the 18 GCMS shape vectors (Fig. 1) visualized in Fig. 2. The Cosine similarity matrix is symmetric, which is why, it is represented with a lower triangular array hereinafter referred to as heatmap. Every entry of the heatmap represents the absolute value of the Cosine similarity between two flexible GCMS modes; the diagonal represents the similarity between a mode with itself and is, therefore, of course, one. The first row and the first column correspond to ${}^f\phi_1^{11}$; increasing the row or column index of the heatmap corresponds to an increase of the indices of ${}^f\phi_m^{kl}$ in the following manner:

1. $l = 1 \rightarrow 3$ for every k and m
 2. $k = 1 \rightarrow 3$ for every m
 3. $m = 1 \rightarrow N_m$
- } see Eq. (36) for the formal index mapping expression

The GCMS shape vectors in Fig. 1 are displayed in the exact same order, see Fig. 1(b) to (j) and (l) to (t), and so are the columns of the hypothetical example in Eq. (1).

Fig. 2 proves that the by inspection of Fig. 1 identified dependencies, see the second paragraph of this section, indeed fulfil condition (35). Such heatmaps are used for the rest of the analysis to identify directly proportional columns of Φ_f .

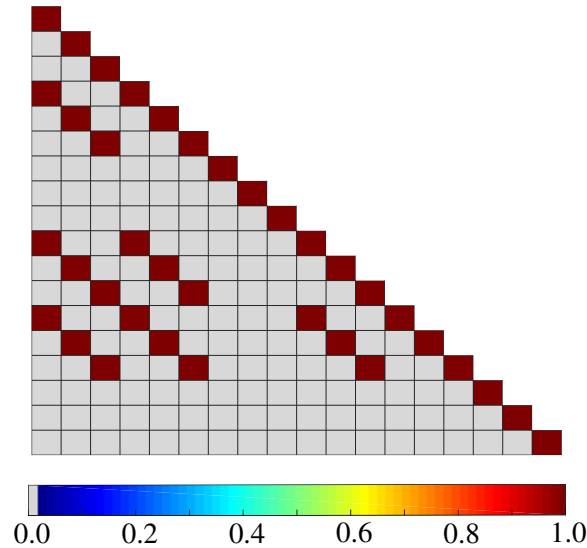


Fig. 2: Absolute value of the Cosine similarity according to Eq. (35) of the first 18 flexible GCMS shape vectors ${}^f\phi_m^{kl}$ of the square-sectioned beam-like example visualized in Fig. 1; displayed as a lower triangular matrix due to symmetry.

This example shows the importance of the mode selection process. The systematic investigation of the flexible GCMS modes, which has not been addressed in the available literature, is not only required to obtain a solvable system of equations, but enables a further reduction of the GCMS coordinates and therefore a gain in efficiency.

⁴For a square-sectioned beam model where the first two bending modes are included in the reduction basis.

4 Dependencies of flexible GMCS reduction matrix

4.1 Detailed analysis of a square-sectioned extruded body

It is clear from the introductory example of Sec. 3.3 that some linear dependencies between flexible GCMS modes are obvious, for example, it is intuitive that linear dependencies between the GCMS shape vectors obtained from the repeated mode pair (Fig. 1(a) and (k)) exist, since the displacements of the nodes in the 1- and 2- directions of ϕ_1 and ϕ_2 are simply “exchanged”. However, this is in general, of course, not the case. This section exhibit that linear dependencies of flexible GCMS shape vectors cannot be identified a priori.

Therefore, a flexible reduction basis is generated from a selection of eight eigenmodes of a 100 mm square-sectioned beam; all the beam-like models subsequently discussed share the following properties and dimensions [10]: Young’s modulus $E = 1.5\text{Pa}$, Poisson’s ratio $\mu = 0.3$, density $\rho = 1000\text{kgm}^{-2}$ and length $l = 2\text{m}$. 20-noded hexahedrals and 15-noded wedge elements (if necessary) were used for the FE discretization. The flexible reduction basis chosen for the analysis includes the first four bending modes, i.e. the first two bending mode shapes in two perpendicular directions (hereinafter distinguished with an asterisk*), as well as the first two torsion and longitudinal eigenmodes, see Fig. 3, which leads to 72 flexible GCMS shape vectors contained in Φ_f with $\text{cond}(\Phi_f) = 2.97 \times 10^6$. In contrast, the condition number of the matrix including the eight original displacement normalized eigenmodes of vibration (Fig. 3) obtained by a FE solver is equal to 1.00. The high condition number of Φ_f indicates that the flexible GCMS shape vectors are not independent, which may be also seen in the Cosine similarity matrix visualized in Fig. 4; the figure depicts the absolute value of the Cosine similarity (Eq. (35)) of two flexible GCMS shape vectors in turn, as already described in more detail in Sec. 3.3. The last 18 columns show, of course, the same pattern and therefore the same dependencies as Fig. 2, i.e. ${}^f\phi_m^{1l} \propto {}^f\phi_m^{2l}$ with $m = B1, B1^*$ and $l = 1, 2, 3$. Not surprisingly, the repeated mode pair of the second bending mode shape (Fig. 3(e) and (f)) shows the same pattern as the first one, i.e. ${}^f\phi_m^{1l} \propto {}^f\phi_m^{2l}$ with $m = B2, B2^*$ and $l = 1, 2, 3$, compare columns 37 to 54 with 55 to 72 in Fig. 4.

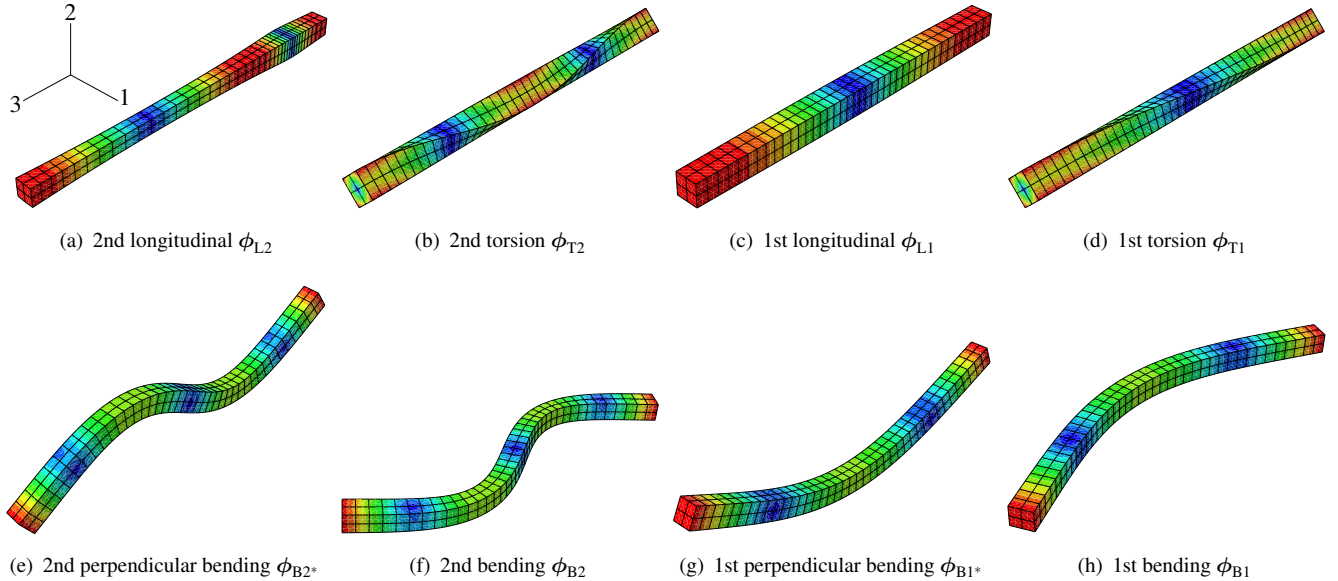


Fig. 3: Selected eigenmodes of vibration ϕ_m of a square-sectioned beam, displayed in the order they appear in the flexible part Φ_f of the GCMS reduction matrix Φ . The contour plots indicate the magnitude of the nodal displacement.

Fig. 4 also reveals that it is possible that linear dependencies between different kinds of modes arise. Columns 28 to 36 indicate that there is a strong dependence ($|c_{ij}| = 0.995$) between the displacement in the 2- and 1-direction of the 1st torsion mode and the displacement in the 3-direction of the 1st bending and perpendicular bending mode, respectively, i.e. ${}^f\phi_{T1}^{2l} \propto {}^f\phi_{B1}^{3l}$ and ${}^f\phi_{T1}^{1l} \propto {}^f\phi_{B1^*}^{3l}$, with $l = 1, 2, 3$. Likewise, there is a correlation, though less significant ($|c_{ij}| = 0.979$), between the displacement in the 3-direction of the 2nd longitudinal mode

and the displacements in the 1- and 2-directions of the first bending mode pair, i.e. ${}^f\phi_{L2}^{3l} \propto {}^f\phi_m^{kl}$ with $m = B1, B1^*$ and $l = 1, 2, 3$. Note, since we are dealing with numerical experiments only, a Cosine similarity (absolute) value below 0.950 may be considered as extremely low, which is why, only dark red entries in the Cosine similarity matrix are important and discussed.

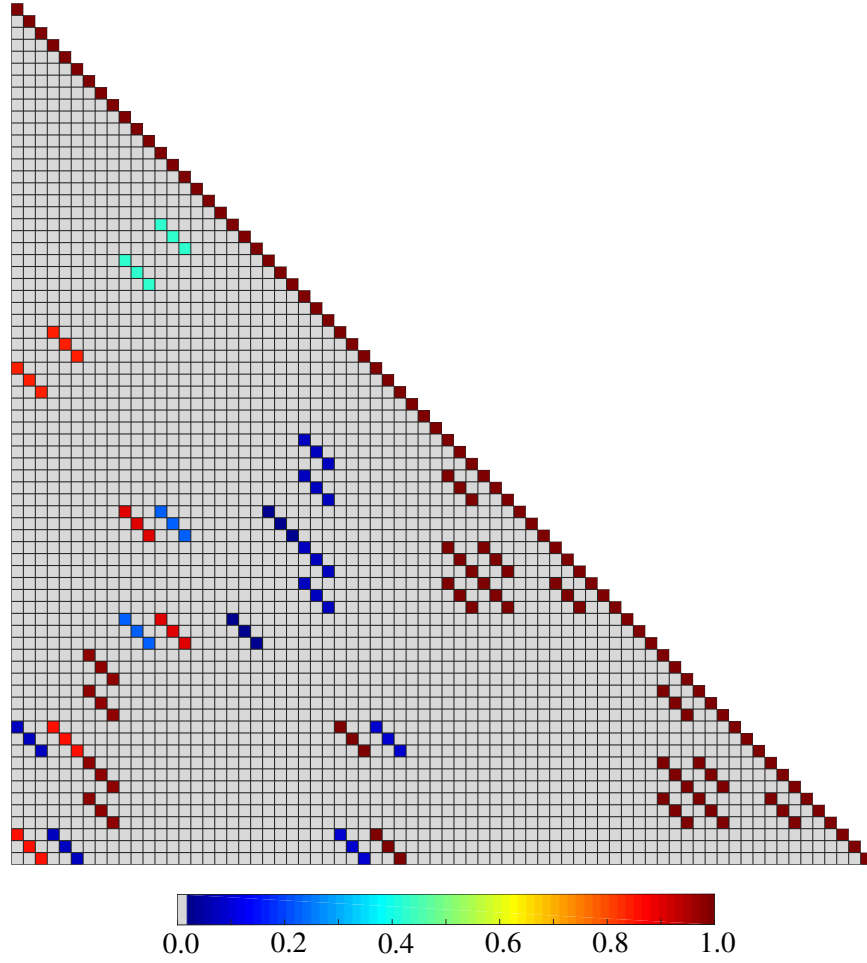


Fig. 4: Absolute value of the Cosine similarity according to Eq. (35) of the flexible GCMS shape vectors ${}^f\phi_m^{kl}$ generated from the eigenmode selection displayed in Fig. 3 of a 100 mm square-sectioned beam; displayed as a lower triangular matrix due to symmetry. The first nine columns and rows correspond to the eigenmode depicted in Fig. 3a, the following nine to the eigenmode of Fig. 3b, and so forth, see Eq. (36).

After the linear dependencies are identified it is important to deal with them appropriately. One way to improve the condition of the flexible reduction basis is to exclude one of the GCMS shape vectors involved in each correlation. This is not only probably the simplest way to handle linear dependencies, but has the advantage that the set of generalized coordinates is reduced by the number of excluded GCMS shape vectors, which leads to a further improvement of the efficiency of the formulation. The only drawback is that one has to determine a threshold value of the Cosine similarity⁵ c_{th} ; the GCMS shape vectors are considered to be linearly dependent if $|c_{ij}| \geq c_{th}$. This may be an iterative process, that continues as long as the condition number is as low as desired, which depends on the problem to be analysed and on the system matrices, or until removing correlated columns does not improve the condition number further (Fig. 5). Fig. 5(a) shows the matrix condition number of the flexible reduction matrix $\text{cond}(\Phi_f)$ generated from the eight eigenmodes of vibration displayed in Fig. 3 over the threshold value c_{th} of the Cosine similarity. Fig. 5(b) depicts the corresponding number of removed columns of Φ_f over c_{th} . The figures indicate that a threshold value relatively close to one ($c_{th} = 0.999$) suffices to reduce the condition number by three orders of magnitude; such a sharp drop can be generally expected if columns are directly proportional as evident

⁵Note, it is unlikely that $|c_{ij}|$ is exactly equal to one, since we are dealing with numerical vectors.

from a series of numerical experiments. Further reducing the threshold ($c_{\text{th}} = 0.995$) leads to a minor improvement by a factor of approximately two. After that, the condition number remains constant within the considered range and removing more columns (from 24 to 27 at $c_{\text{th}} = 0.980$) does not lower the condition number further. Hence, “convergence” of $\text{cond}(\Phi_f)$ should be always checked prior time integration to avoid numerical errors, if not, $c_{\text{th}} = 0.993$ is suggested to avoid unacceptable high condition numbers.

The initial threshold value c_{th}^0 may be chosen to be one, or as the Cosine similarity (absolute) value calculated from a pair of GCMS shape vectors where linear dependence is a priori known, which is, for example, the case between the GCMS shape vectors obtained from ϕ_{B1} and ϕ_{B1^*} (Fig. 3). Hence, one can define

$$c_{\text{th}}^0 := \frac{\langle \phi_{B1}^l, \phi_{B1^*}^l \rangle}{|\phi_{B1}^l| |\phi_{B1^*}^l|} \quad \text{for any } l = 1, 2, 3, \quad (37)$$

for the here considered example.

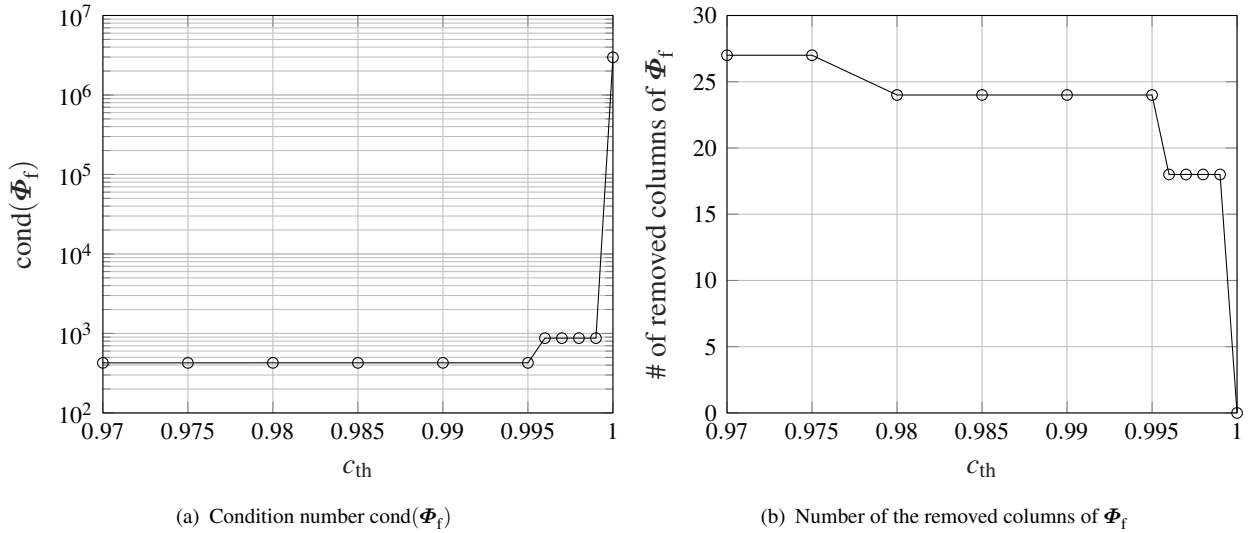


Fig. 5: Condition number of the flexible GCMS reduction matrix, generated from the eigenmodes of the square-sectioned beam displayed in Fig. 3, and the number of the removed columns of Φ_f over the threshold value of the Cosine similarity c_{th} .

4.2 Extruded bodies with different cross-sections

The analysis of Sec. 4.1 was also conducted for bodies with the same properties, as outlined in the second paragraph of the section, and with the same eigenmodes included in the reduction basis, see Fig. 3, but with different cross-sections, see Fig. 6. The main findings are summarized in the following paragraphs.

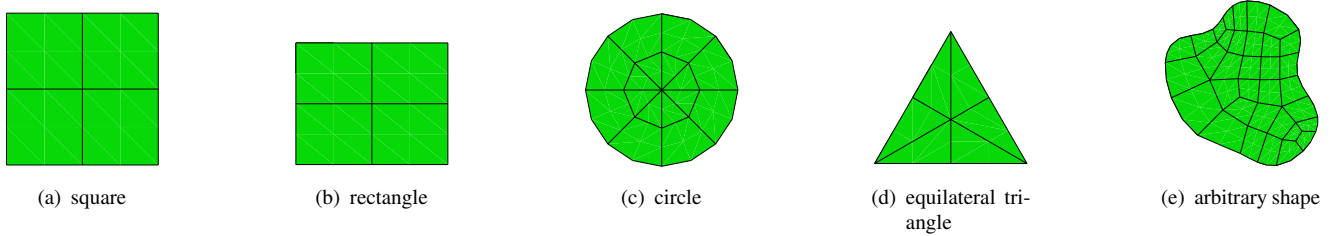


Fig. 6: Different cross-sections with FE mesh of the beam-like models used to analyse the linear dependencies of the flexible reduction matrix Φ_f (scale 1:5).

The condition number of the flexible reduction matrices of the analysed beams ranges from the order of 10^5 to 10^{11} , where the “best” condition number belongs to the arbitrary beam (Fig. 6(e)) and the “worst” one to the

circular beam (Fig. 6(c)). This clearly emphasises the importance of the present investigations, since one has to expect to loose eleven digits of accuracy on top of all the other errors, such as finite machine precession, if the linear dependencies are not handled appropriately. Removing linearly dependent modes with a Cosine similarity higher than $c_{th} = 0.993$ lowers the condition number by at least two orders of magnitude. A subsequent scaling of the columns of Φ_f , i.e. converting all flexible GCMS shape vectors to the same norm/length, lowers $\text{cond}(\Phi_f)$ of all beam-like models down to approximately 10^2 . Scaling is a crucial preprocessing step for the GCMS formulation, as can be seen especially for the circular-sectioned beam, where scaling lowers the condition number by seven orders of magnitude!

The exclusion of linearly dependent GCMS shape vectors reduces the initially 72 flexible GCMS coordinates by 33% in the best case and by at least 25%, even though only eight eigenmodes of vibration are included in the flexible reduction basis here. Hence, the gain in efficiency may be essential especially for larger problems. This shows that a neat preprocessing is not only important for accuracy, but also for efficiency, due to the significant reduction of the system DOFs.

The FE meshes for the beam-like models were chosen in order to preserve the lines of symmetry of the cross-sections (Fig. 6), except for the circle, where the infinite number of symmetry lines is reduced to four, due to the discretization. The arbitrary shaped beam (Fig. 6(e)) was generated such that the geometry itself as well as the FE mesh does not exhibit any symmetries. Nevertheless, the GCMS reduction matrices of the circular, the square and the arbitrary shaped beam show exactly the same linear dependencies, except that the correlations between the 1st torsion mode and the 1st bending mode pair, see the 3rd paragraph of Sec. 4.1, are slightly stronger for the square beam. Also, the Cosine similarity matrix of the arbitrary shaped beam show additionally some very weak correlations, yet with negligible values. Therefore, it seems that “small” deviations from symmetric geometries as well as the design of FE meshes have a minor influence on the linear dependencies of flexible GCMS reduction matrices and that not the shape but the number of symmetry lines dictates the linear dependencies. Finally, the rectangular and equilateral triangular beam exhibit the same correlations as the square beam, except the linear dependencies within each GCMS mode set generated from the bending modes, see the second paragraph of Sec. 3.3.

5 Dependencies between the flexible and the rigid body motion part of the reduction matrix

It is still possible that the condition number of the total reduction matrix $\text{cond}(\Phi)$ is unacceptably high after the exclusion of linearly dependent flexible GCMS modes identified with the Cosine similarity. This happens whenever a column of Φ is a linear combination of others, i.e. if Eq. (28) is fulfilled with more than two vectors involved. Such dependencies usually arise between the flexible Φ_f and rigid body motion part $[\Phi_t \ \Phi_r]$ of the reduction basis. The Cosine similarity fails to identify such linear combinations, which is why, we have to resort to the SVD, briefly introduced in Sec. 3.2.2, to determine the nullspace of Φ . The nullspace identifies the GCMS shape vectors involved in linear combinations. Therefore, we can iteratively (1) identify $\text{null}(\Phi)$, (2) remove one of the flexible GCMS shape vectors involved, since the rigid body motion shape vectors must be kept in the reduction basis, and (3) start with (1) again as long as the condition number is as low as desired.

As mentioned in Sec. 3.2.2, it is in general required to distinguish between vanishing⁶ and non-vanishing singular values σ_i to determine the nullspace of a matrix. However, there is a sharp drop (two orders of magnitude or more) visible in the plot of the singular values of Φ , see Fig. 7, if linear dependencies exist. Fig. 7 shows the singular values σ_i of the unmodified GCMS reduction matrix Φ of the circular beam-like model (Fig. 6(c)) in descending order; the especially distinctive singular value drop by almost six orders of magnitude occurs for the depicted example between the 72nd and 73rd singular value. The vanishing singular values after the drop indicate that Eq. (28) is fulfilled for non-zero coefficients a_p^i , i.e. the components of the right singular vectors v_i of Φ , see Sec. 3. If Φ_f is already well-conditioned (Cosine similarity preconditioning), linear dependencies between

⁶In this context, vanishing means small compared to large singular values.

the rigid body motion and flexible part of the reduction matrix exist. Hence, linear dependencies between Φ_f and $[\Phi_t \ \Phi_r]$ manifest themselves as a sharp drop between two subsequent singular values, which is why, no threshold for vanishing singular values needs to be determined, i.e. right singular vectors corresponding to singular values after the drop (here, 73 to 84) compose the nullspace of Φ , see Eq. (31). The corresponding right singular vectors indicate the columns of Φ involved in linear dependencies; these dependencies may be cancelled if one of the involved GCMS shape vectors of Φ_f is excluded.

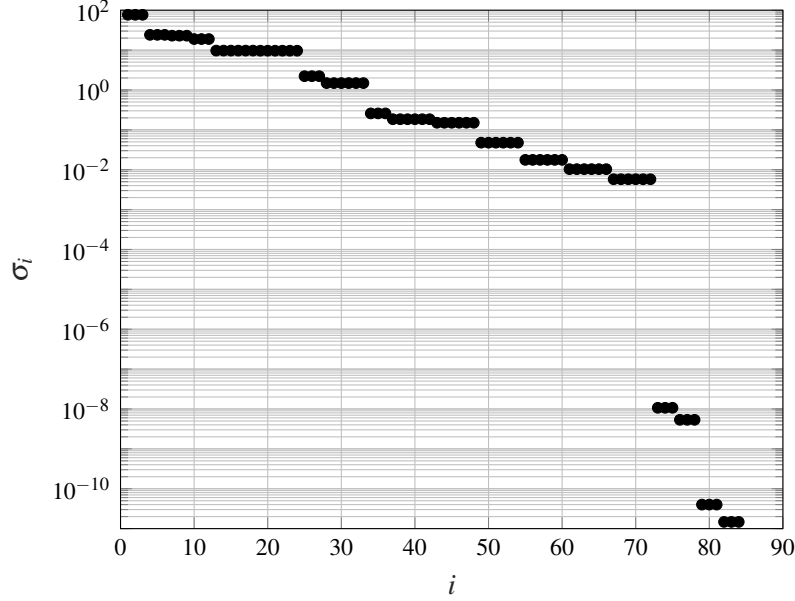


Fig. 7: Singular values σ_i of the unmodified GCMS reduction matrix Φ of the circular beam-like model (Fig. 6(c)) in descending order.

For all analysed beam-like models (Fig. 6), $\text{cond}(\Phi)$ is one order of magnitude larger than the condition number of the reduced⁷ and scaled flexible reduction matrix Φ_f . Note, it is not possible to scale the rotational part Φ_r of the reduction matrix, however, it is highly recommended to ensure that the GCMS shape vectors have similar norms. Which is why, the translational and flexible GCMS shape vectors are scaled to the mean value of the norms of the columns of Φ_r , which lowers the overall condition number of the already preconditioned (Cosine similarity, SVD) matrix Φ again down to the order of 10^2 .

Note, if linear dependencies arise, always a full set of three flexible GCMS shape vectors ${}^f\phi_m^{kl}$ with $k = 1, 2, 3$, see Eq. (6), must be removed, since the number of GCMS coordinates q must be a multiple of three such that the introduction of A_{bd} is feasible, see Sec. 2.2.

⁷The reduced flexible reduction matrix is the matrix Φ_f , where the directly proportional columns identified via the Cosine similarity are removed.

6 Analysis of a crankshaft – a relevant engineering example

The previously analysed beam-like examples (Sec. 4 and Sec. 5) appear less often in practical applications, which is why, this section is devoted to the analysis of a crankshaft of a reciprocal two-cylinder combustion engine. The crankshaft was discretized with 31999 10-noded tetrahedrals yielding 50289 nodes in total. The first twelve eigenmodes of vibration, covering the frequency range up to 10000 Hz, are included in the flexible reduction basis and are visualized in Fig. 8.

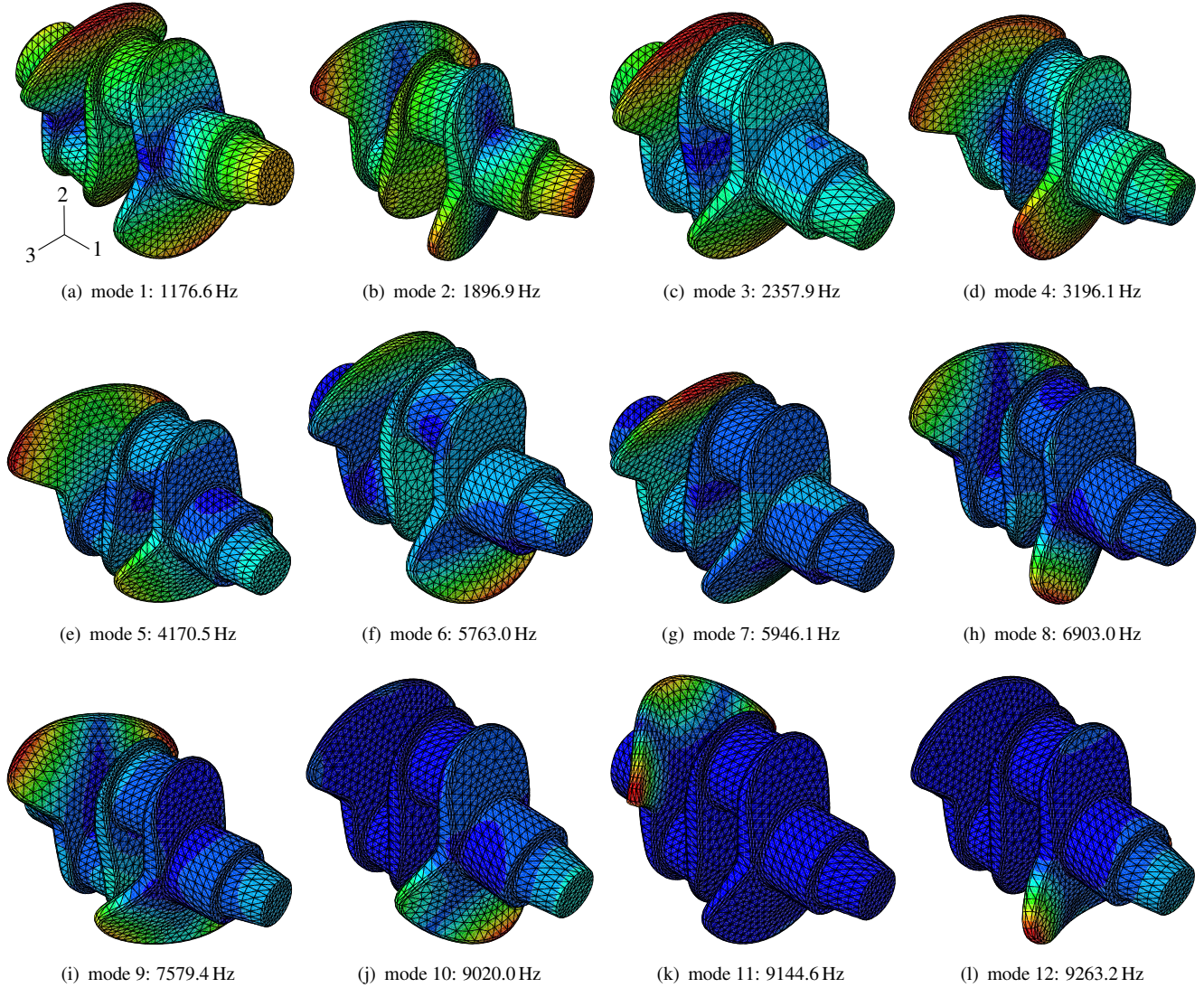


Fig. 8: First twelve displacement normalized eigenmodes of vibration of the analysed crankshaft of a reciprocal two-cylinder combustion engine; the contour plots indicate the magnitude of the nodal displacement.

The Cosine similarity matrix of Φ_f obtained from the crankshafts' eigenmodes of vibration is depicted in Fig. 9. The only dark-red entries are present in the upper corner of the lower triangular array with Cosine similarity values of approximately 0.97, which is considered too low to exclude shape vectors involved in these correlations. Hence, there are no directly proportional modes in the flexible reduction matrix, which is, therefore, relatively well-conditioned with $\text{cond}(\Phi_f)$ in the order of 10^2 .

In addition, there is no significant drop in the singular values σ_i of Φ , as shown in Fig. 10. Numerical experiments showed that the drop after σ_9 by one order of magnitude is not caused by linear combinations between the flexible and rigid body motion part of Φ , i.e. no improvement in $\text{cond}(\Phi)$ is reached if the right singular vectors v_i with $i > 9$ are considered to be in $\text{null}(\Phi)$ and the “pretended” linear combinations are removed via column

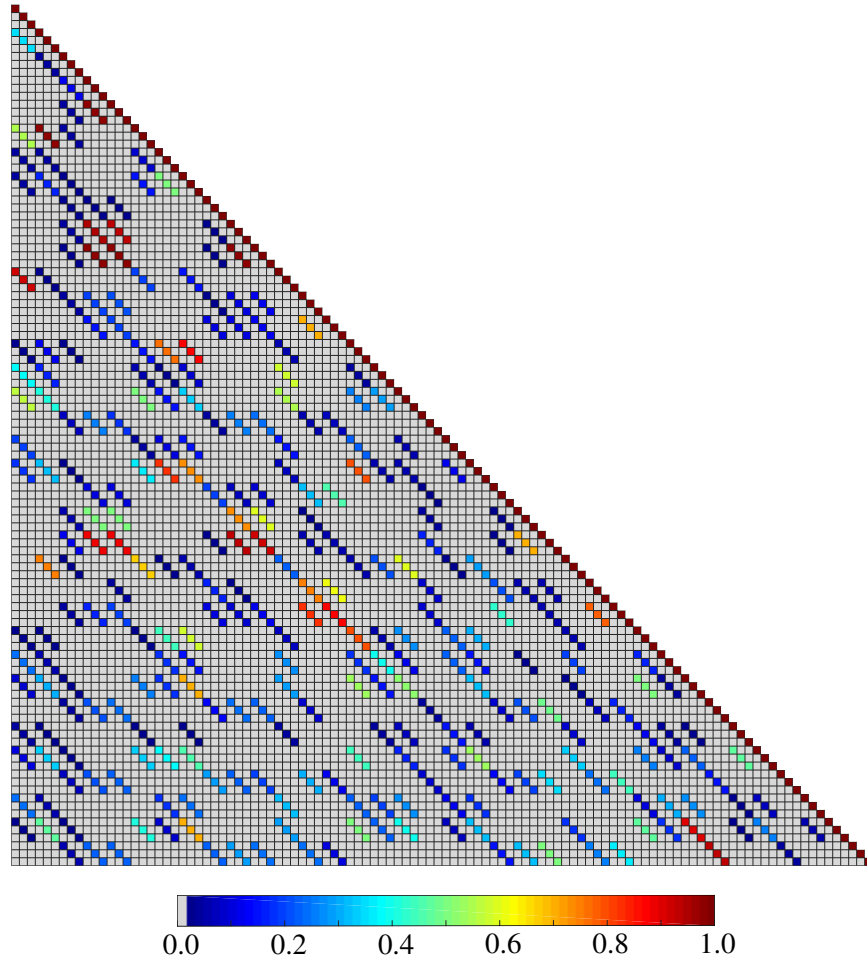


Fig. 9: Absolute value of the Cosine similarity according to Eq. (35) of the flexible GCMS shape vectors ${}^f\phi_m^{kl}$ generated from the eigenmode selection displayed in Fig. 8 of a crankshaft; displayed as a lower triangular matrix due to symmetry. The first nine columns and rows correspond to the eigenmode depicted in Fig. 8(a), the following nine to the eigenmode of Fig. 8(b), and so forth.

exclusion. The condition number of the total reduction matrix Φ of the crankshaft is in the order of 10^4 , in contrast to the condition number of approximately 1.40 of the eigenmodes of vibration matrix generated from the modes depicted in Fig. 8. However, scaling of the translational and flexible GCMS shape vectors to the mean value of the norms of the rotational GCMS modes, lowers the overall condition number of the GCMS reduction matrix Φ of the crankshaft down to the order of 10^2 .

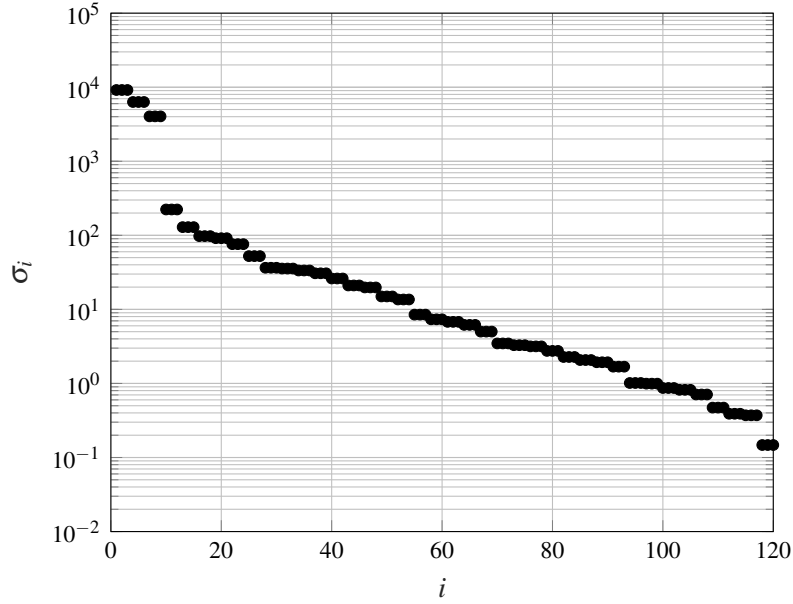


Fig. 10: Singular values σ_i of the unmodified GCMS reduction matrix Φ of the analysed crankshaft (Fig. 8) in descending order.

7 Step by step strategy to handle linear dependencies of the reduction matrix

The algorithm shown below states a strategy how to handle linear dependencies within the reduction matrix Φ of the GCMS formulation and has proved itself useful in practice:

```

Data: ill-conditioned  $\Phi$ 
Result: well-conditioned  $\Phi$ 
extract  $\Phi_t, \Phi_r, \Phi_f$  from  $\Phi$ 
scale the columns of  $\Phi_t$  and  $\Phi_f$  to the mean value of the norms of the columns of  $\Phi_r$ 
calculate  $\text{cond}(\Phi)$ 
if  $\text{cond}(\Phi)$  is larger than desired then
    calculate the strictly lower triangular Cosine similarity matrix  $c_{ij}$  of  $\Phi_f$ 
    if  $|c_{ij}| \geq c_{th}$  then
        | remove  $i$ -th column of  $\Phi_f$  for unique  $i$ 
    end
    reassemble  $\Phi$  and calculate  $\text{cond}(\Phi)$ 
    if  $\text{cond}(\Phi)$  is still larger than desired then
        calculate the SVD of  $\Phi$ 
        while big drop between singular values, i.e.  $\sigma_i > 10^2 \sigma_{i+1}$  do
            | remove one of the  $\phi_m^{kl}$  involved in linear dependencies as indicated by  $v_{i+1}$ 
            | calculate the SVD of  $\Phi$ 
        end
    end
    return preconditioned  $\Phi$ 
else
    | return scaled  $\Phi$ 
end

```

Algorithm 1: Pseudocode to handle linear dependencies of Φ and to improve $\text{cond}(\Phi)$.

Note, the SVD is an expensive operation especially for large matrices. However, one may calculate the SVD of the small (compared to Φ) upper triangular matrix R obtained by the QR decomposition of Φ to efficiently calculate the desired right singular vectors and singular values. This is feasible, since Φ and R share the same right singular vectors and singular values and the left singular vectors are not needed here.

8 Conclusions

The present paper identified and resolved the weakness of the GCMS formulation, i.e. a in many cases ill-conditioned reduction matrix, which may introduce large errors (condition numbers up to nearly 10^{18}) or even lead to unsolvable problems if not handled appropriately. The ill-conditioned reduction matrix is caused by linear dependencies of GCMS shape vectors (the matrix's columns) generated from original linearly independent FE eigenmodes of vibration and undeformed nodal coordinates; the first 18 GCMS shape vectors of a FE model are visualized to contribute to a better understanding of the GCMS modes. It has been shown by numerical experiments of simple extruded bodies with different cross-sections that such linear dependencies may also arise for fully asymmetric geometries and FE meshes, which is why, it is impossible to identify linearly dependent GCMS shape vectors a priori. It was shown how the SVD, the matrix condition number and the Cosine similarity may be used to identify and eliminate these linear dependencies by column exclusion, yielding not only a sufficiently well-conditioned system, but also a smaller number of flexible GCMS coordinates (DOFs) and therefore a further gain in efficiency. The Cosine similarity was employed to identify directly proportional columns of the flexible part and the SVD for the remaining linear combinations between the flexible and rigid body motion part of the reduction matrix. The crankshaft example suggests that complex real-world engineering systems are potentially less likely to result in ill-conditioned GCMS reduction matrices, however, a neat preprocessing is suggested in any case to avoid unexpected errors. Furthermore, it has been revealed that the norm, which may be arbitrary chosen for the flexible and translational part, of the GCMS vectors can have a substantial influence on the overall condition number, which is why, it is highly recommended to ensure that the GCMS modes have similar norms. A step-by-step preprocessing procedure has been derived to handle the linear dependencies within the GCMS reduction matrix and to improve its condition number.

Further research should be conducted to answer the question whether it is beneficial (in terms of accuracy of the solution) to remove GCMS shape vectors as long as the condition number is close to one, which is the case for classical reduction matrices containing the eigenmodes of vibration, or to remove highly correlated GCMS modes only and accept a higher condition number.

References

- [1] A. Pechstein, D. Reischl, and J. Gerstmayr, "A generalized component mode synthesis approach for flexible multibody systems with a constant mass matrix," *Journal of Computational and Nonlinear Dynamics*, vol. 8, no. 1, pp. 011019/1–011019/10, 2013.
- [2] A. A. Shabana, *Dynamics of Multibody Systems*. Cambridge: Cambridge University Press, 4th ed., 2013.
- [3] M. C. C. Bampton and R. R. Craig Jr., "Coupling of substructures for dynamic analyses," *American Institute of Aeronautics and Astronautics Journal*, vol. 6, no. 7, pp. 1313–1319, 1968.
- [4] M. Borga, *Learning Multidimensional Signal Processing*. PhD thesis, Linköping University, 581 83 Linköping, Sweden, 1998. No. 531.
- [5] M. Geradin and D. J. Rixen, *Mechanical Vibrations - Theory and Application to Structural Dynamics*. New York: John Wiley & Sons, 3rd ed., 2015.
- [6] J. Gerstmayr and J. A. C. Ambrósio, "Component mode synthesis with constant mass and stiffness matrices applied to flexible multibody systems," *International Journal for Numerical Methods in Engineering*, vol. 73, no. 11, pp. 1518–1546, 2008.
- [7] J. Gerstmayr and J. Schöberl, "A 3d finite element method for flexible multibody systems," *Multibody System Dynamics*, vol. 15, no. 4, pp. 305–320, 2006.
- [8] M. Schörgenhuber, A. Humer, and J. Gerstmayr, "Efficient fluid-structure interaction based on modally reduced multibody systems and smoothed particle hydrodynamics," in *Proceedings of the WCCM XI, ECCM V and ECFD VI*, July 20–25, Barcelona, Spain 2014.

- [9] P. Ziegler, A. Humer, A. Pechstein, and J. Gerstmayr, "Generalized component mode synthesis for the spatial motion of flexible bodies with large rotations about one axis," *ASME Journal of Computational and Nonlinear Dynamics*, vol. 11, no. 4, pp. 041018; 10 pages, 2016.
- [10] R. G. Winkler, D. Plakomytis, and J. Gerstmayr, "A null space projection approach for modally reduced flexible multi-body systems," in *ASME Proceedings of the IDETC/CIE Conference*, vol. 6: 12th International Conference on MSNDC, pp. V006T09A022; 9 pages, August 21-24, Charlotte, NC, USA, 2016.
- [11] A. Humer, F. Naets, W. Desmet, and J. Gerstmayr, "A generalized component mode synthesis approach for global modal parameterization in flexible multibody dynamics," in *Proceedings of the 3rd Joint International Conference on Multibody System Dynamics*, June 29 – July 3, Busan, Korea, 2014.
- [12] C. Lanczos, *The Variational Principles of Mechanics*. New York: Dover Publications Inc., 4th ed., 2012.
- [13] O. C. Zienkiewicz and R. L. Taylor, *The Finite Element Method: The basis*, vol. 1. Oxford: Butterworth-Heinemann, 5th ed., 2000.
- [14] L. N. Trefethen and D. B. III, *Numerical Linear Algebra*. Philadelphia: Society for Industrial and Applied Mathematics, 1997.
- [15] N. M. Newmark, "A method of computation for structural dynamics," *ASCE Journal of the Engineering Mechanics Division*, vol. 85, no. 3, pp. 67–94, 1959.